NASA Technical Memorandum 100663

RECENT ADVANCES IN TRANSONIC COMPUTATIONAL AEROELASTICITY

JOHN T. BATINA
ROBERT M. BENNETT
DAVID A. SEIDEL
HERBERT J. CUNNINGHAM
SAMUEL R. BLAND

SEPTEMBER 1988

NASA
National Aeronautics and Space Administration

Langley Research Center
Hampton, Virginia 23665-5225

RECENT ADVANCES IN TRANSONIC COMPUTATIONAL AEROELASTICITY

John T. Batina
Robert M. Bennett
David A. Seidel
Herbert J. Cunningham
Samuel R. Bland

NASA Langley Research Center
Hampton, Virginia 23665-5225

Abstract

A transonic unsteady aerodynamic and aeroelasticity code called CAP-TSD has been developed for application to realistic aircraft configurations. The code permits the calculation of steady and unsteady flows about complete aircraft configurations for aeroelastic analysis in the flutter critical transonic speed range. The CAP-TSD code uses a time-accurate approximate factorization (AF) algorithm for solution of the unsteady transonic small-disturbance potential equation. The paper gives an overview of the CAP-TSD code development effort and presents results which demonstrate various capabilities of the code. Calculations are presented for several configurations including the General Dynamics one-ninth scale F-16C aircraft model and the ONERA M6 wing. Calculations are also presented from a flutter analysis of a 45° sweptback wing which agree well with the experimental data. The paper presents descriptions of the CAP-TSD code and algorithm details along with results and comparisons which demonstrate these recent developments in transonic computational aeroelasticity.

Notation

b_o reference length, $c_r/2$

c, c_r airfoil chord and wing reference chord, respectively

C_p pressure coefficient

k	reduced frequency, $\omega c_r/2U$
M	freestream Mach number
t	time, nondimensionalized by freestream speed and wing reference chord
U	freestream speed
α_0, α_1	mean angle of attack and amplitude of pitch oscillation, respectively
γ	ratio of specific heats
Δt	nondimensional time step
$\bar{\eta}$	fractional semispan
μ	ratio of wing mass to mass of air in the truncated cone that encloses the wing
ρ	freestream flow density
ϕ	disturbance velocity potential
ω, ω_α	angular frequency and natural frequency of the first torsion mode, respectively

Subscripts

t	tail
w	wing

Introduction

Presently, considerable research is being conducted to develop finite-difference computer codes for calculating transonic unsteady aerodynamics for aeroelastic applications [1]. These computer codes are being developed to provide accurate methods of calculating unsteady airloads for the prediction of aeroelastic phenomena such as flutter and divergence. For example, the CAP-TSD [2] unsteady transonic small-disturbance (TSD) code was recently developed for transonic aeroelastic analyses of complete aircraft configurations. The name CAP-TSD is an

acronym for Computational Aeroelasticity Program - Transonic Small Disturbance. The new code permits the calculation of unsteady flows about complete aircraft for aeroelastic analysis in the flutter critical transonic speed range. The code can treat configurations with arbitrary combinations of lifting surfaces and bodies including canard, wing, tail, control surfaces, tip launchers, pylons, fuselage, stores, and nacelles. Steady and unsteady pressure comparisons were presented for numerous cases which demonstrated the geometrical applicability of CAP-TSD [2-3]. These calculated results were generally in good agreement with available experimental pressure data which validated CAP-TSD for multiple component applications with mutual aerodynamic interference effects. Aeroelastic applications of CAP-TSD were presented by Cunningham, et al. [4] and Bennett, et al. [5] for simple well-defined wing cases. The cases were selected as a first step toward performing aeroelastic analyses for complete aircraft configurations. The calculated flutter boundaries compared well with the experimental data for subsonic, transonic, and supersonic freestream Mach numbers, which gives confidence in CAP-TSD for aeroelastic prediction.

The CAP-TSD code uses a time-accurate approximate factorization (AF) algorithm recently developed by Batina [6] for solution of the unsteady TSD equation. The AF algorithm involves a Newton linearization procedure coupled with an internal iteration technique. The algorithm was shown to be efficient for application to steady or unsteady transonic flow problems. It can provide accurate solutions in only several hundred time steps, yielding a significant computational cost savings when compared to alternative methods. For reasons of practicality and affordability, an efficient algorithm and a fast computer code are requirements for realistic aircraft applications.

Recently, several algorithm modifications have been made which have improved the stability of the AF algorithm and the accuracy of the results [7,8]. These algorithm modifications

include: (1) an Engquist-Osher (E-O) type-dependent switch to more accurately and efficiently treat regions of supersonic flow, (2) extension of the E-O switch for second-order-accurate spatial differencing in supersonic regions to improve the accuracy of the results, (3) nonisentropic effects to more accurately treat cases with strong shocks, and (4) nonreflecting far field boundary conditions for more accurate unsteady applications. The work has been a major research activity over the past two and one-half years within the Unsteady Aerodynamics Branch at NASA Langley Research Center. The purpose of the paper is to give an overview of the CAP-TSD code development effort and report on the recent algorithm changes and code improvements. The paper documents these developments and presents results which demonstrate these recent advances in transonic computational aeroelasticity.

Transonic Small Disturbance Equation

The flow is assumed to be governed by the general frequency modified TSD potential equation which may be written as

$$M^2 (\phi_t + 2\phi_x)_t = [(1 - M^2)\phi_x + F\phi_x^2 + G\phi_y^2]_x + (\phi_y + H\phi_x\phi_y)_y + (\phi_z)_z \qquad (1)$$

Several choices are available for the coefficients F, G, and H depending upon the assumptions used in deriving the TSD equation. For transonic applications, the coefficients are herein defined as

$$F = -\frac{1}{2}(\gamma + 1) M^2, \quad G = \frac{1}{2}(\gamma - 3) M^2, \quad H = -(\gamma - 1) M^2 \qquad (2)$$

The linear potential equation is recovered by simply setting F, G, and H equal to zero.

Entropy and vorticity modifications to TSD theory, to treat cases with strong shock waves, have been developed as described by Batina [8]. These modifications include: (1) an alternative streamwise flux in the TSD equation which was derived by an asymptotic expansion of the Euler equations, (2) a modified velocity vector defined as the sum of potential and rotational parts which in turn modified the streamwise flux, and (3) the calculation and convection of entropy throughout the flow field. The modified theory includes the effects of entropy and vorticity while retaining the relative simplicity and cost efficiency of the TSD formulation [8].

Approximate Factorization Algorithm

A time-accurate approximate factorization algorithm was developed [6-8] to solve the unsteady TSD equation including entropy and vorticity effects. In this section, the AF algorithm is briefly described.

General Description

The AF algorithm consists of a Newton linearization procedure coupled with an internal iteration technique. For unsteady flow calculations, the solution procedure involves two steps. First, a time linearization step is performed to determine an estimate of the potential field. Second, internal iterations are performed to minimize linearization and factorization errors. Specifically, the TSD equation is written in general form as

$$R\,(\phi^{n+1}) = 0 \qquad (3)$$

where ϕ^{n+1} represents the unknown potential field at time level (n+1). The solution to Eq. (3) is then given by the Newton linearization of Eq. (3) about ϕ^{*}

$$R(\phi^*) + \left(\frac{\partial R}{\partial \phi}\right)_{\phi=\phi^*} \cdot \Delta\phi = 0 \qquad (4)$$

In Eq. (4), ϕ^* is the currently available value of ϕ^{n+1} and $\Delta\phi = \phi^{n+1} - \phi^*$. During convergence of the iteration procedure, $\Delta\phi$ will approach zero so that the solution will be given by $\phi^{n+1} = \phi^*$. In general, only one or two iterations are required to achieve acceptable convergence.

Mathematical Formulation

The AF algorithm is formulated by first approximating the time-derivative terms by second-order-accurate finite-difference formulae. The TSD equation is rewritten by substituting $\phi = \phi^* + \Delta\phi$ and neglecting squares of derivatives of $\Delta\phi$ (which is equivalent to applying Eq. (4) term by term). The resulting equation is then rearranged and the left-hand side is approximately factored into a triple product of operators yielding

$$L_\xi L_\eta L_\zeta \Delta\phi = -\sigma R(\phi^*, \phi^n, \phi^{n-1}, \phi^{n-2}) \qquad (5)$$

where the operators L_ξ, L_η, L_ζ and residual R were derived and presented in Ref. [6]. In Eq. (5) σ is a relaxation parameter which is normally set equal to 1.0. To accelerate convergence to steady-state, the residual R may be over-relaxed using $\sigma > 1$. Equation (5) is solved using three sweeps through the grid by sequentially applying the operators L_ξ, L_η, L_ζ as

$$\xi\text{ - sweep: } L_\xi \bar{\Delta\phi} = -\sigma R \qquad (6a)$$

$$\eta \text{ - sweep: } L_\eta \, \bar{\bar{\Delta\phi}} = \bar{\Delta\phi} \tag{6b}$$

$$\zeta \text{ - sweep: } L_\zeta \, \Delta\phi = \bar{\bar{\Delta\phi}} \tag{6c}$$

The AF algorithm uses an Engquist-Osher (E-O) type-dependent switch to change the spatial differencing from central differencing in regions of subsonic flow to upwind differencing in regions of supersonic flow. This, of course, allows for the correct numerical description of the physical domain of dependence. The E-O switch is based on sonic reference conditions and does not admit expansion shocks as part of the solution. Use of the E-O switch also generally increases computational efficiency because of the larger time steps which may be taken. Furthermore, the E-O switch of the AF algorithm has been recently extended for second-order spatial accuracy in supersonic regions of the flow. Details of these developments are reported by Batina [7].

Boundary Conditions

The flow tangency boundary conditions are imposed along the mean plane of the respective lifting surfaces and the wakes are assumed to be planar extensions from the trailing edges to the downstream boundary of the finite-difference grid. The numerical implementation of these conditions [2] allows for coplanar as well as non-coplanar combinations of horizontal (canard, wing, horizontal tail, launchers) and vertical (pylons, vertical tail) surfaces. Bodies such as the fuselage, stores, and nacelles are treated using simplified boundary conditions on a prismatic surface rather than on the true surface [2]. The method is consistent with the small-disturbance approximation and treats bodies with sufficient accuracy to obtain the correct global effect on the flow field without the use of special grids or complicated coordinate

transformations. This type of modeling is similar to that of Boppe and Stern [9] where good agreement was shown in comparison with experimental data for configurations with a fuselage and flow-through nacelles.

For unsteady applications, nonreflecting far field boundary conditions similar to those of Whitlow [10] are used. The nonreflecting conditions absorb most of the waves that are incident on the grid boundaries and consequently allow the use of smaller computational grids. These boundary conditions are consistent with the AF solution procedure and are described in more detail by Batina [7].

Aeroelastic Solution

In this section the aeroelastic computational procedures are described including the equations of motion and the time-marching solution.

Equations of Motion

The aeroelastic equations of motion are based on a right-hand orthogonal coordinate system with the x-direction defined as positive downstream and the z-direction positive upward [4]. The presentation herein is limited to the case of an isolated wing with motion in the z-direction from an undisturbed position in the z = 0 plane. The equations of motion may be written as

$$M\ddot{q} + C\dot{q} + Kq = Q \qquad (7)$$

where q is a vector of generalized displacements, M is the generalized mass matrix, C is the damping matrix, K is the stiffness matrix, and Q is the vector of generalized aerodynamic forces.

Time-Marching Solution

The aeroelastic solution procedure for integrating Eq. (7) is similar to that described by Edwards, et al. [11]. Reference [11] describes for a two-dimensional, two-degree-of-freedom system an aeroelastic solution in terms of a state equation formulation. By a parallel formulation, a linear state equation is developed from Eq. (7) which is solved numerically using the modified state-transition matrix integrator of Ref. [11]. This integrator was shown to be superior to six alternative structural integration algorithms [12].

For aeroelastic analysis, two steps are generally required in performing the calculations. In the first step, the steady-state flow field is calculated to account for wing thickness, camber, and mean angle of attack thus providing the starting flow field for the aeroelastic analysis. The second step is to prescribe an initial disturbance to begin the structural integration. Disturbance velocities in one or more modes, rather than displacements, have been found to be distinctly superior in avoiding nonphysical, strictly numerical transients and their possible associated instabilities. In determining a flutter point, the freestream Mach number M and the associated freestream speed U are usually held fixed. A judiciously chosen value of the dynamic pressure $\rho U^2/2$ is used to compute the free decay transients. These resulting transients of the generalized coordinates are analyzed for their content of damped or growing sine-waves, with the rates of growth or decay indicating whether the dynamic pressure is above or below the flutter value. This analysis then indicates whether to increase or decrease the value of dynamic pressure in subsequent runs to determine a neutrally stable result.

CAP-TSD Code

The AF algorithm is the basis of the CAP-TSD code for transonic unsteady aerodynamic and aeroelastic analysis of realistic aircraft configurations. The present capability has the option of

half-span modeling for symmetric cases or full-span modeling to allow the treatment of antisymmetric mode shapes, fuselage yaw, or unsymmetric configurations such as an oblique wing or unsymmetric wing stores. In the present coding of the AF algorithm, the time derivatives are implemented for variable time stepping to allow for step-size cycling to accelerate convergence to steady state. Also, since the L_ξ, L_η, and L_ζ operators only contain derivatives in their respective coordinate directions, all three sweeps of the solution procedure have been fully vectorized.

Results and Discussion

Results are presented for several configurations including the General Dynamics one-ninth scale F-16C aircraft model [13,14], the ONERA M6 wing [15], and a 45° sweptback wing [16, 17], to demonstrate various capabilities of the CAP-TSD code.

General Dynamics F-16C Aircraft Model Results

To demonstrate application of CAP-TSD to a realistic aircraft configuration, results were obtained for the General Dynamics one-ninth scale F-16C aircraft model. Shown in Fig. 1 are the F-16C components that are modeled using CAP-TSD. The F-16C is modeled using four lifting surfaces and two bodies. The lifting surfaces include: (1) the wing with leading and trailing edge control surfaces, (2) the launcher, (3) a highly-swept strake, aft strake, and shelf surface, and (4) the horizontal tail. The bodies include: (1) the tip missile, and (2) the fuselage. In these calculations, the freestream Mach number was M = 0.9 and the aircraft was at 2.38° angle of attack. Also, the leading edge control surface of the wing was deflected upwards 2° for comparison with the experimental steady pressure data of Ref. [14]. These steady pressure comparisons are made to assess the accuracy of CAP-TSD for complete airplane

applications. There are no unsteady experimental data to validate the CAP-TSD code for time accurate F-16C calculations. Nonetheless, an unsteady calculation was performed to demonstrate the time-accurate capability. For simplicity, the results were obtained for a rigid pitching motion where the entire F-16C aircraft was forced to oscillate about the model moment reference axis at a reduced frequency of $k = 0.1$. The oscillation amplitude was chosen as $\alpha_1 = 0.5°$, and 300 steps per cycle of motion were computed corresponding to $\Delta t = 0.1047$. Parallel results were also obtained for the wing alone to investigate the aerodynamic interference effects of the additional aircraft components on wing unsteady pressures.

Steady pressure comparisons for the F-16C aircraft model are presented in Fig. 2 for three span stations of the wing and one span station of the tail. For this case, there is a moderately strong shock wave on the upper surface of the wing and the CAP-TSD pressures agree well with the experimental pressures. For the tail, the flow is predominantly subcritical and the CAP-TSD pressures again agree well with the experimental data.

Unsteady pressure distributions along the wing and tail upper surfaces are shown in Fig. 3 for the entire F-16C aircraft undergoing a rigid pitching motion. These unsteady pressure results are presented at the same span stations as the steady-state results (Fig. 2). Two sets of calculated pressures are compared corresponding to complete airplane and wing alone modeling. As shown in Fig. 3, there is a relatively large shock pulse in the real part of the wing upper surface pressures due to the motion of the shock wave. This shock pulse is of larger magnitude and is located further downstream in the complete airplane model. These features are attributed to a stronger steady-state shock on the upper surface of the wing produced by the accelerated flow about the fuselage and the launcher/tip missile. For the tail, the unsteady pressures are relatively small in comparison with the wing pressures and thus were plotted on an expanded scale. The tail is located considerably aft of the pitch axis and thus its motion is plunge

dominated which results in smaller airloads for the low value of k considered. Furthermore, these pressures are nearly 90° out of phase with the aircraft motion since the real components are small compared to the imaginary components.

ONERA M6 Wing Results

To test the entropy and vorticity modifications to TSD theory, applications were performed for the ONERA M6 wing [15]. The M6 wing has an aspect ratio of 3.8, a leading edge sweep angle of 30°, and a taper ratio of 0.562. The airfoil section of the wing is the ONERA "D" airfoil which is a 10% maximum thickness-to-chord ratio symmetric section. Pressures were calculated at M = 0.92 with the wing at 0° mean angle of attack. These conditions correspond to an AGARD test case for assessment of inviscid flow field methods [15] and were selected for comparison with the tabulated Euler results of Rizzi contained therein.

Calculations were performed using: (a) unmodified TSD theory and (b) TSD with entropy and vorticity effects. Steady pressure distributions along three span stations ($\bar{\eta}$ = 0.08, 0.47, and 0.82) of the wing are presented in Fig. 4 from both solutions. For this case, the flow is symmetric about the wing with shocks on the upper and lower surfaces. As shown in Fig. 4(a), the results from the unmodified TSD theory compare well with the Euler results in predicting the leading edge suction peak and the overall pressure levels. However, the shock is located too far aft and is too strong outboard near the tip in comparison with the Euler calculation. When the entropy and vorticity modifications are included in the calculation, the shock is displaced forward from the previous solution, as shown in Fig. 4(b). Here the shock location and shock strength are in very good agreement with the Euler results at all three span stations on the wing. Consequently, the steady pressure distributions from the modified TSD theory now compare very well with the Euler pressures.

Wing Flutter Results

To assess the CAP-TSD code for flutter applications, a simple well-defined wing case was selected as a first step toward performing aeroelastic analyses for complete aircraft configurations [4,5]. The wing being analyzed is a semispan wind-tunnel-wall-mounted model that has a quarter-chord sweep angle of 45°, a panel aspect ratio of 1.65, and a taper ratio of 0.66 [16]. The wing is an AGARD standard aeroelastic configuration which was tested in the Transonic Dynamics Tunnel (TDT) at NASA Langley Research Center [17]. A planview of the wing is shown in Fig. 5. The wing has a NACA 65A004 airfoil section and was constructed of laminated mahogany. In order to obtain flutter for a wide range of Mach number and density conditions in the TDT, holes were drilled through the wing to reduce its stiffness. To maintain the aerodynamic shape of the wing, the holes were filled with a rigid foam plastic. The wing is modeled structurally using the first four natural vibration modes which are illustrated in Fig. 6. These modes which are numbered 1 through 4 represent first bending, first torsion, second bending, and second torsion, respectively, as determined by a finite element analysis. The modes have natural frequencies which range from 9.6 Hz for the first bending mode to 91.54 Hz for the second torsion mode.

Flutter calculations were performed for the 45° sweptback wing using CAP-TSD to assess the code for aeroelastic applications. Two sets of results are presented corresponding to: (1) using the linear potential equation ($F = G = H = 0$) and modeling the wing aerodynamically as a flat plate (zero thickness) and (2) using the complete (nonlinear) TSD equation and including wing thickness. The first set of results allows for direct comparison with parallel linear theory calculations performed using the FAST subsonic kernel function program [18]. The second set of results more accurately models the wing geometry as well as the flow physics. All of the results are compared with the experimental flutter data of Yates, et al. [17] which spans

the range, $0.338 \leq M \leq 1.141$.

Comparisons of flutter characteristics from the linear calculations with the experimental data are given in Fig. 7. The flutter speed index (defined as $U/(b_o \omega_\alpha \sqrt{\mu})$) as a function of freestream Mach number is shown in the figure. The experimental flutter data defines a typical transonic flutter "dip" with the bottom near M = 1.0 for this case. The bottom of the dip in flutter speed index was defined by the approach to the M = 1.072 flutter point during the wind tunnel operation. Results from the CAP-TSD (linear) code are presented at twelve values of M covering the entire Mach number range over which the flutter data was measured. Results from the FAST program are presented for the limited range $0.338 \leq M \leq 0.96$ since the method is restricted to subsonic freestreams. Overall, the linear CAP-TSD results compare well with the experimental data for subsonic as well as supersonic Mach numbers. Note that the subsonic FAST results are also in good agreement with the data. Such a result is not unexpected for this very thin wing of moderate sweep and taper at zero angle of attack. It does indicate that the wing properties are well-defined for benchmark purposes.

In the subsonic Mach number range, the CAP-TSD and FAST calculations predict a slightly unconservative flutter speed, except at M = 0.338, by as much as 2% (Fig. 7) in comparison with the experimental data. In general though, the linear CAP-TSD results agree well with the FAST results. The good agreement in this three-way correlation between experiment, linear theory, and CFD flutter results gives confidence in the CAP-TSD code for flutter prediction.

Comparisons of flutter characteristics from the linear and nonlinear CAP-TSD calculations with the experimental data are also given in Fig. 7. Three flutter points are plotted from the nonlinear CAP-TSD calculations corresponding to M = 0.678, 0.901, and 0.96. Comparisons between the two sets of CAP-TSD results show differences due to wing thickness and nonlinear effects. With increasing Mach number these differences become larger. For example, at M =

0.678, 0.901, and 0.96, the flutter speed index decreased by 1%, 5%, and 19%, respectively. The decrease in flutter speed at M = 0.901 is largely due to including wing thickness since there are no supersonic points in the flow at this condition. The decrease in flutter speed at M = 0.96 is attributed to both wing thickness and nonlinear effects since an embedded supersonic region of moderate size was detected in the wing tip region. The nonlinear CAP-TSD results at both M = 0.901 and 0.96 are slightly conservative in comparison with the experimental flutter speed index values. Nonetheless, the nonlinear CAP-TSD flutter results compare favorably with the experimental data, which is the first step toward validating the code for general transonic aeroelastic applications.

Concluding Remarks

A transonic unsteady aerodynamic and aeroelasticity code called CAP-TSD has been developed for application to realistic aircraft configurations. The code permits the calculation of unsteady flows about complete aircraft configurations for aeroelastic analysis in the flutter critical transonic speed range. The CAP-TSD code uses a time-accurate approximate factorization (AF) algorithm for solution of the unsteady transonic small-disturbance equation including entropy and vorticity effects. The AF algorithm has been shown to be very efficient for steady or unsteady transonic flow problems. It can provide accurate solutions in only several hundred time steps yielding a significant computational cost savings when compared to alternative methods. For reasons of practicality and affordability, an efficient algorithm and a fast computer code are requirements for realistic aircraft applications.

Results were presented for several configurations including the General Dynamics one-ninth scale F-16C aircraft model and the ONERA M6 wing, to demonstrate various capabilities of the CAP-TSD code. For the F-16C aircraft model, calculated steady pressure distributions

compared well with the experimental data. Unsteady pressures for the entire F-16C aircraft undergoing a rigid pitching motion were also presented. Comparisons with parallel wing alone results revealed aerodynamic interference effects of the additional aircraft components on wing unsteady pressures. These effects emphasize the importance of including all components in the calculation. The CAP-TSD code thus provides the capability of modeling complete aircraft configurations for realistic transonic unsteady aerodynamic and aeroelastic analyses. For the ONERA M6 wing, CAP-TSD results were presented both with and without entropy and vorticity effects. The results obtained by including these effects were in very good agreement with Euler results in terms of predicting the shock location and strength. The CAP-TSD code includes the entropy and vorticity effects while retaining the relative simplicity and cost efficiency of the small-disturbance potential formulation. Therefore, the capability provides the aeroelastician with an affordable method to analyze relatively difficult transonic cases.

Results were also presented from a flutter analysis of a 45° sweptback wing. The flutter boundaries from CAP-TSD (linear) were in agreement with parallel subsonic linear theory results and compared well with the experimental flutter data for subsonic and supersonic freestream Mach numbers. The nonlinear CAP-TSD flutter results also compared favorably with the experimental data which is the first step toward validating the code for general transonic aeroelastic analysis of more complex configurations.

References

1. J. W. Edwards, and J. L. Thomas. Computational Methods for Unsteady Transonic Flows. AIAA Paper No. 87-0107 (1987).

2. J. T. Batina, D. A. Seidel, S. R. Bland, and R. M. Bennett. Unsteady Transonic Flow Calculations for Realistic Aircraft Configurations. AIAA Paper No. 87-0850 (1987).

3. R. M. Bennett, S. R. Bland, J. T. Batina, M. D. Gibbons, and D. G. Mabey. Calculation of Steady and Unsteady Pressures on Wings at Supersonic Speeds with a Transonic Small-Disturbance Code. AIAA Paper No. 87-0851 (1987).

4. H. J. Cunningham, J. T. Batina, and R. M. Bennett. Modern Wing Flutter Analysis by Computational Fluid Dynamics Methods. ASME Paper No. 87-WA/Aero-9 (1987).

5. R. M. Bennett, J. T. Batina, and H. J. Cunningham. Wing Flutter Calculations with the CAP-TSD Unsteady Transonic Small Disturbance Program. AIAA Paper No. 88-2347 (1988).

6. J. T. Batina. An Efficient Algorithm for Solution of the Unsteady Transonic Small-Disturbance Equation. AIAA Paper No. 87-0109 (1987).

7. J. T. Batina. Unsteady Transonic Algorithm Improvements for Realistic Aircraft Applications. AIAA Paper No. 88-0105 (1987).

8. J. T. Batina. Unsteady Transonic Small-Disturbance Theory Including Entropy and Vorticity Effects. AIAA Paper No. 88-2278 (1988).

9. C. W. Boppe, and M. A. Stern. Simulated Transonic Flows for Aircraft with Nacelles, Pylons, and Winglets. AIAA Paper No. 80-0130 (1980).

10. W. Whitlow, Jr. Characteristic Boundary Conditions for Three-Dimensional Transonic Unsteady Aerodynamics. NASA TM 86292 (1984).

11. J. W. Edwards, R. M. Bennett, W. Whitlow, Jr., and D. A. Seidel. Time-Marching Transonic Flutter Solutions Including Angle-of-Attack Effects. Journal of Aircraft, vol. 20, no. 11, 899-906 (1983).

12. J. W. Edwards, R. M. Bennett, W. Whitlow, Jr., and D. A. Seidel. Time-Marching Transonic Flutter Solutions Including Angle-of-Attack Effects. AIAA Paper No. 82-3685 (1982).

13. M. C. Fox, and C. S. Feldman. Model and Test Information Report, 1/9-Scale F-16C and F-16D Force and Loads Model. General Dynamics Report 16PR2179 (1982).

14. C. S. Feldman. Wind Tunnel Data Report, 1/9-Scale F-16C Pressure Loads Test. General Dynamics Report 16PR2252 (1982).

15. H. Yoshihara. Test Cases for Inviscid Flow Field Methods. AGARD-AR-211 (1985).

16. E. C. Yates, Jr. AGARD Standard Aeroelastic Configurations for Dynamic Response. Candidate Configuration 1. - Wing 445.6. NASA TM 100492 (1987).

17. E. C. Yates, Jr., N. S. Land, and J. T. Foughner, Jr. Measured and Calculated Subsonic and Transonic Flutter Characteristics of a 45° Sweptback Wing Planform in Air and in Freon-12 in the Langley Transonic Dynamics Tunnel. NASA TN D-1616 (1963).

18. R. N. Desmarais, and R. M. Bennett. User's Guide for a Modular Flutter Analysis Software System (FAST Version 1.0). NASA TM 78720 (1978).

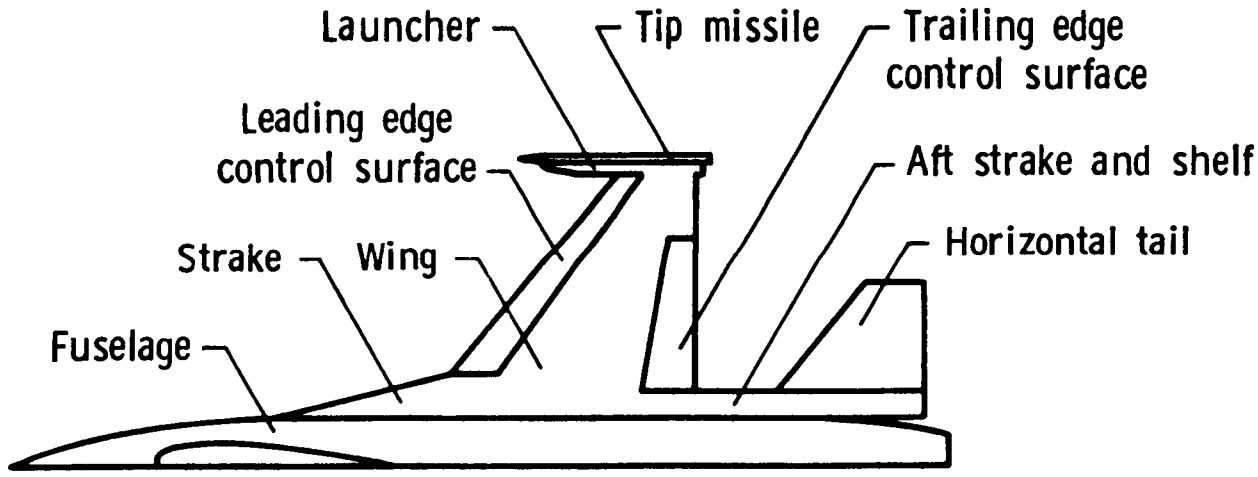

Fig. 1 CAP-TSD modeling of the General Dynamics one-ninth scale F-16C aircraft model.

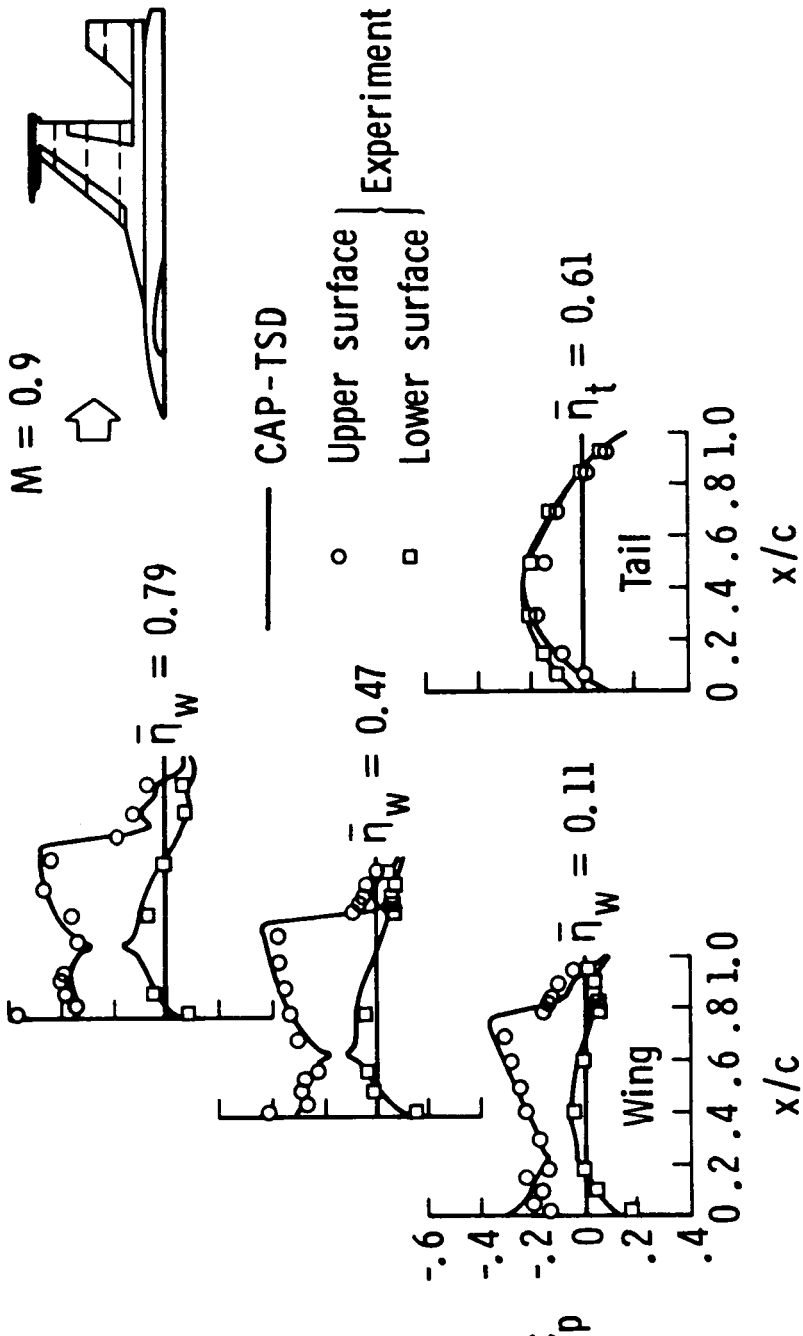

Fig. 2 Comparison between CAP-TSD and experimental steady pressure distributions on the wing and tail of the F-16C aircraft model at M = 0.9 and α_o = 2.38°.

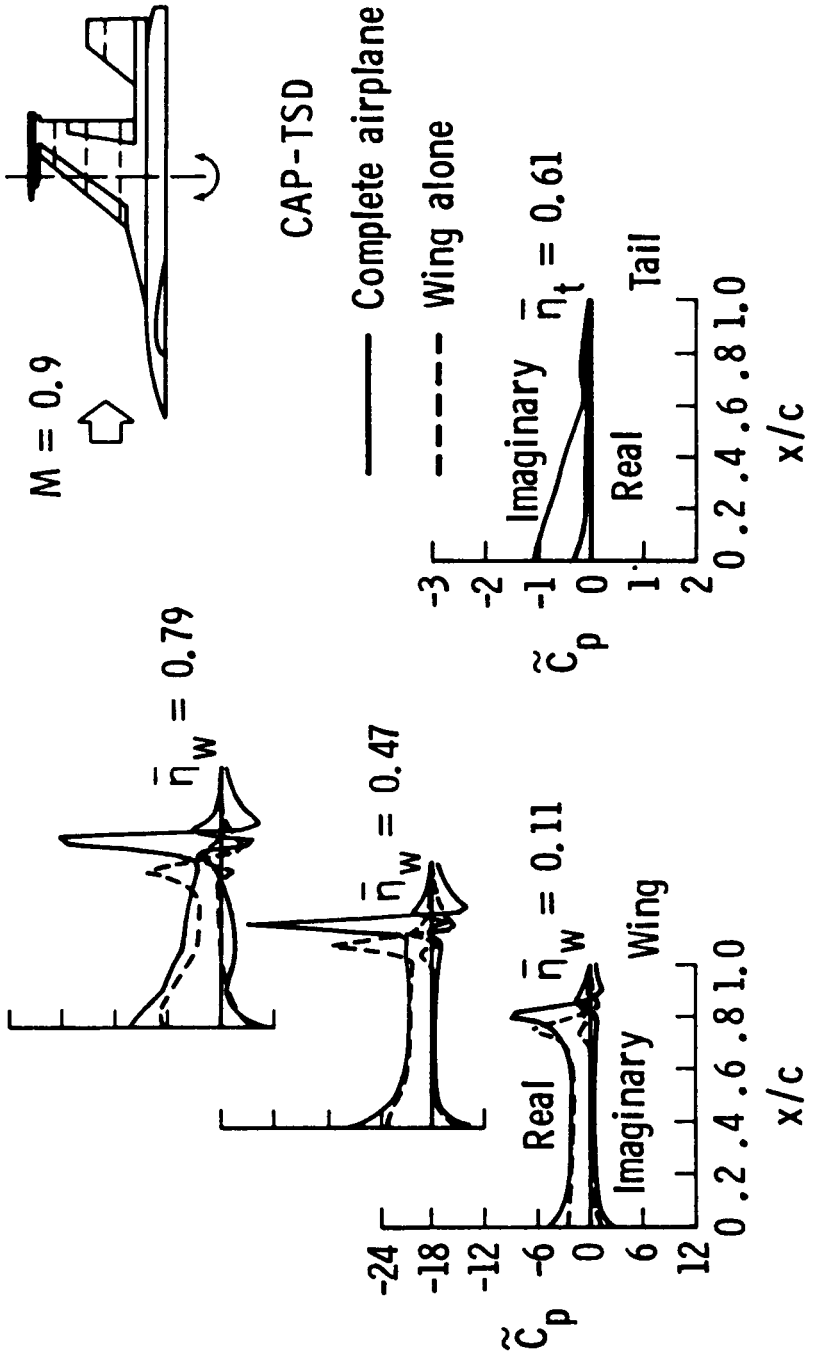

Fig. 3 CAP-TSD unsteady pressure distributions on the wing and tail upper surfaces of the F-16C aircraft model due to complete airplane rigid pitching at M = 0.9, α_o = 2.38°, α_1 = 0.5°, and k = 0.1.

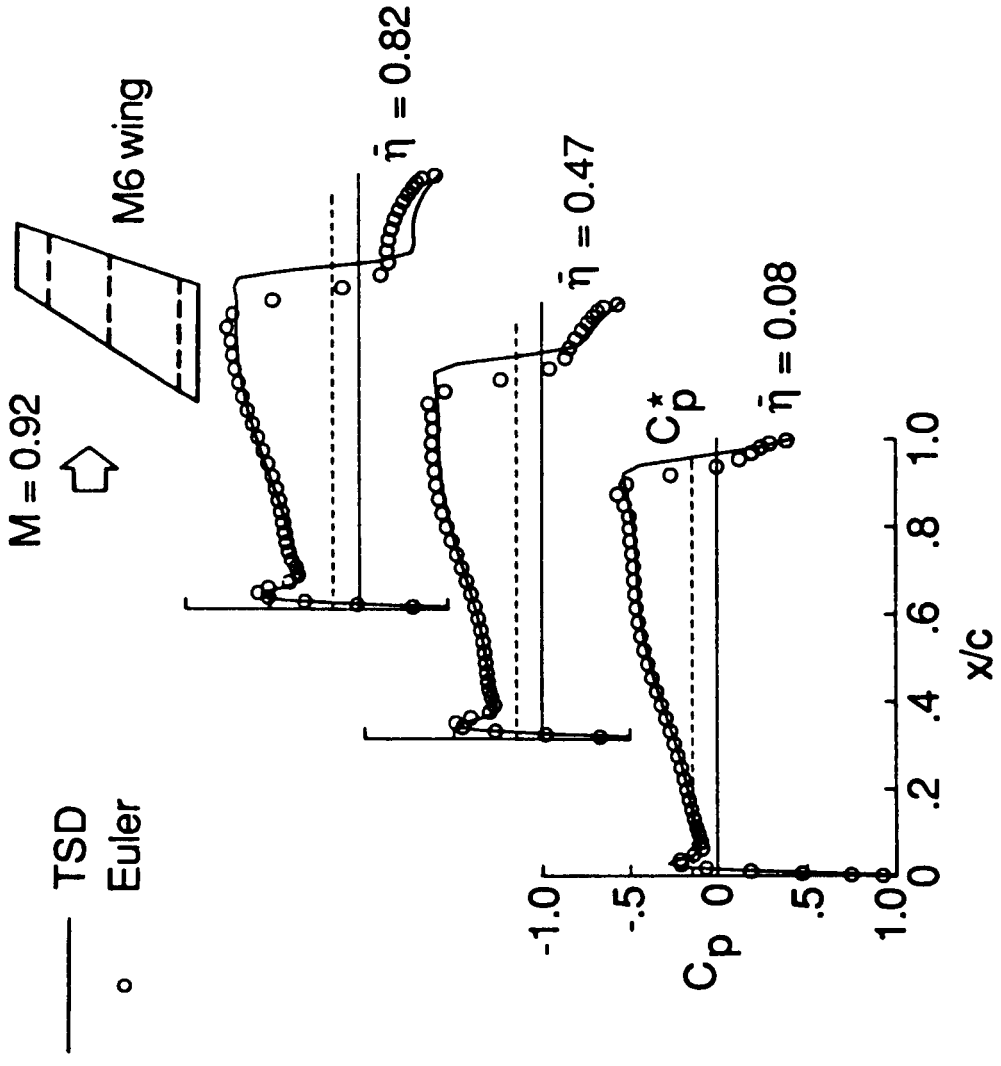

(a) TSD.

Fig. 4 Comparison of steady pressure distributions for the ONERA M6 wing at M = 0.92 and $\alpha_o = 0°$.

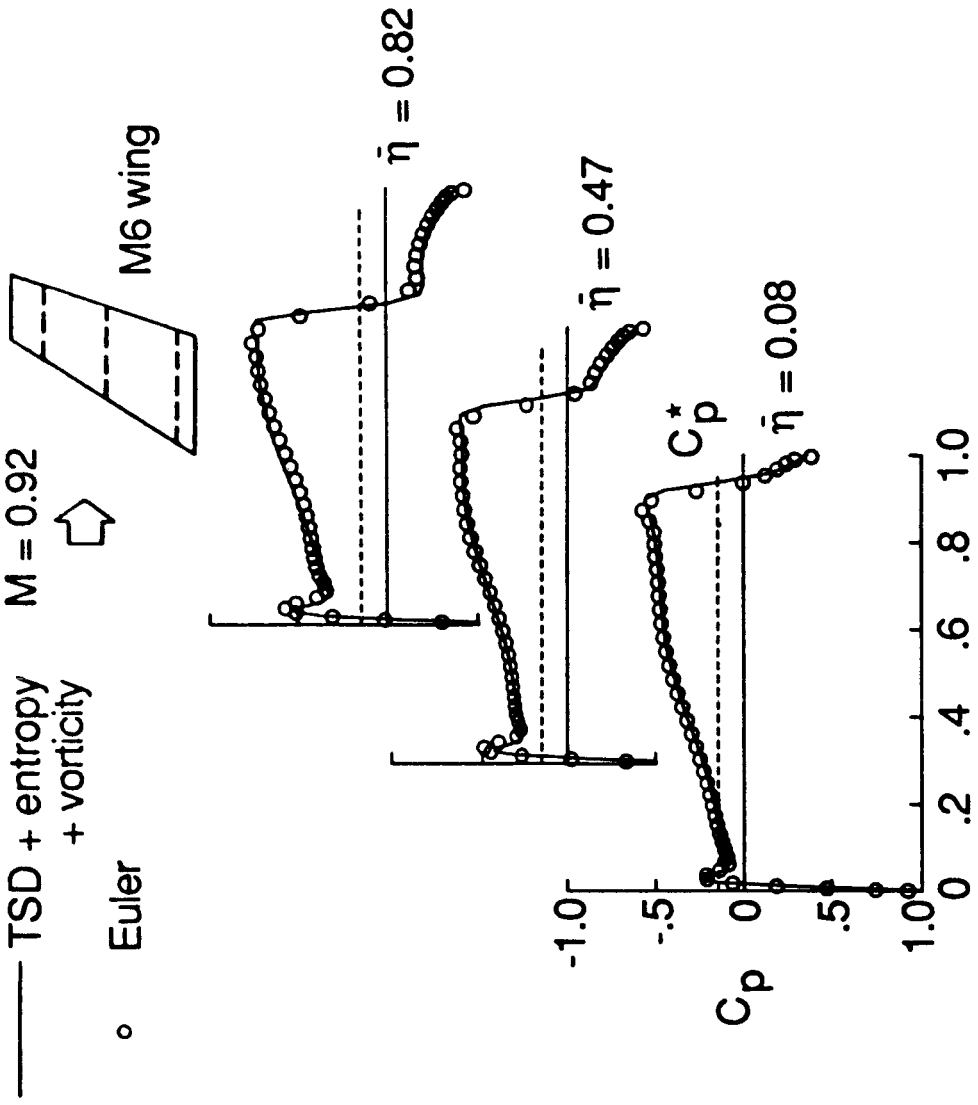

(b) TSD + entropy + vorticity.

Fig. 4 Concluded.

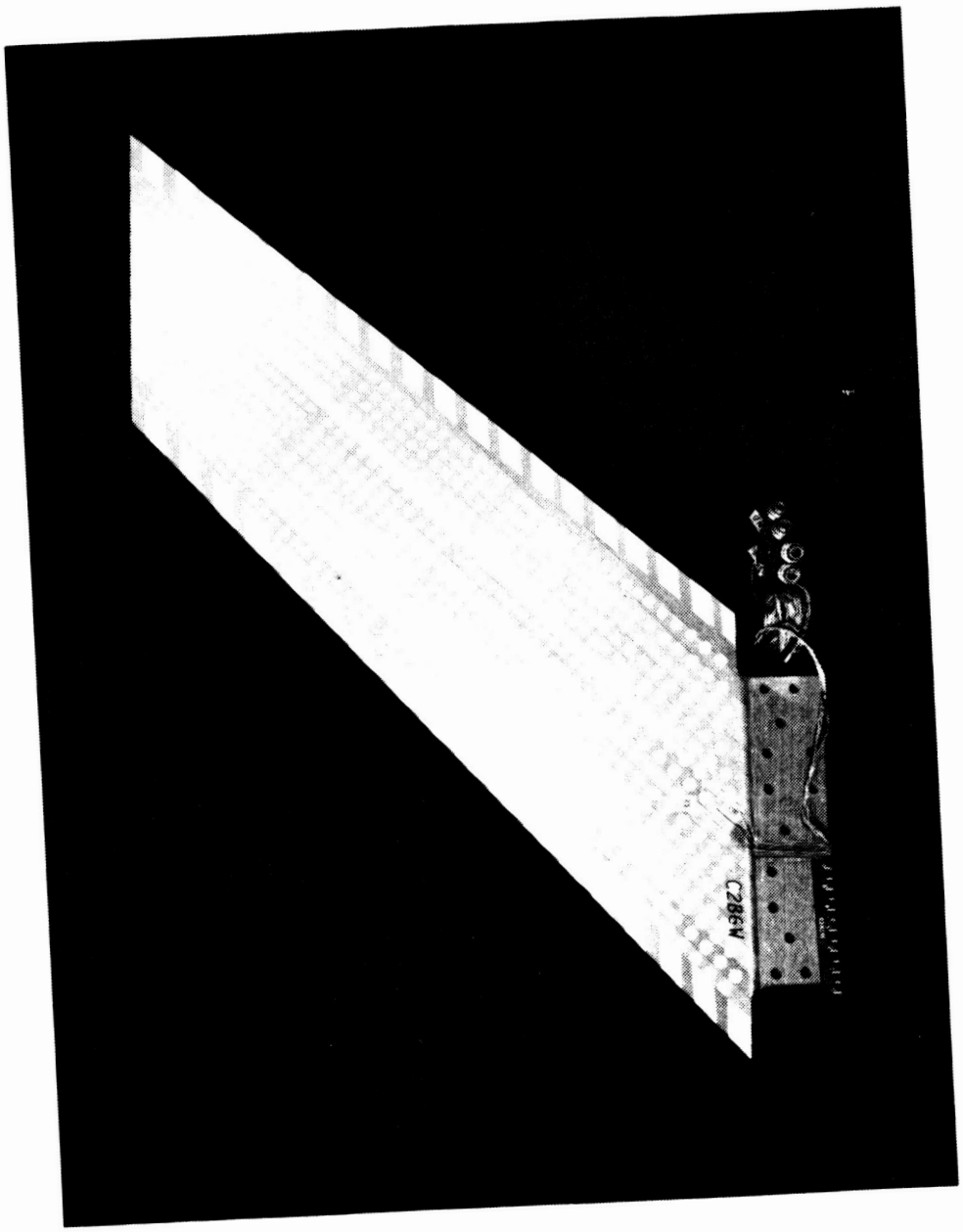

Fig. 5 Planview of 45° sweptback wing.

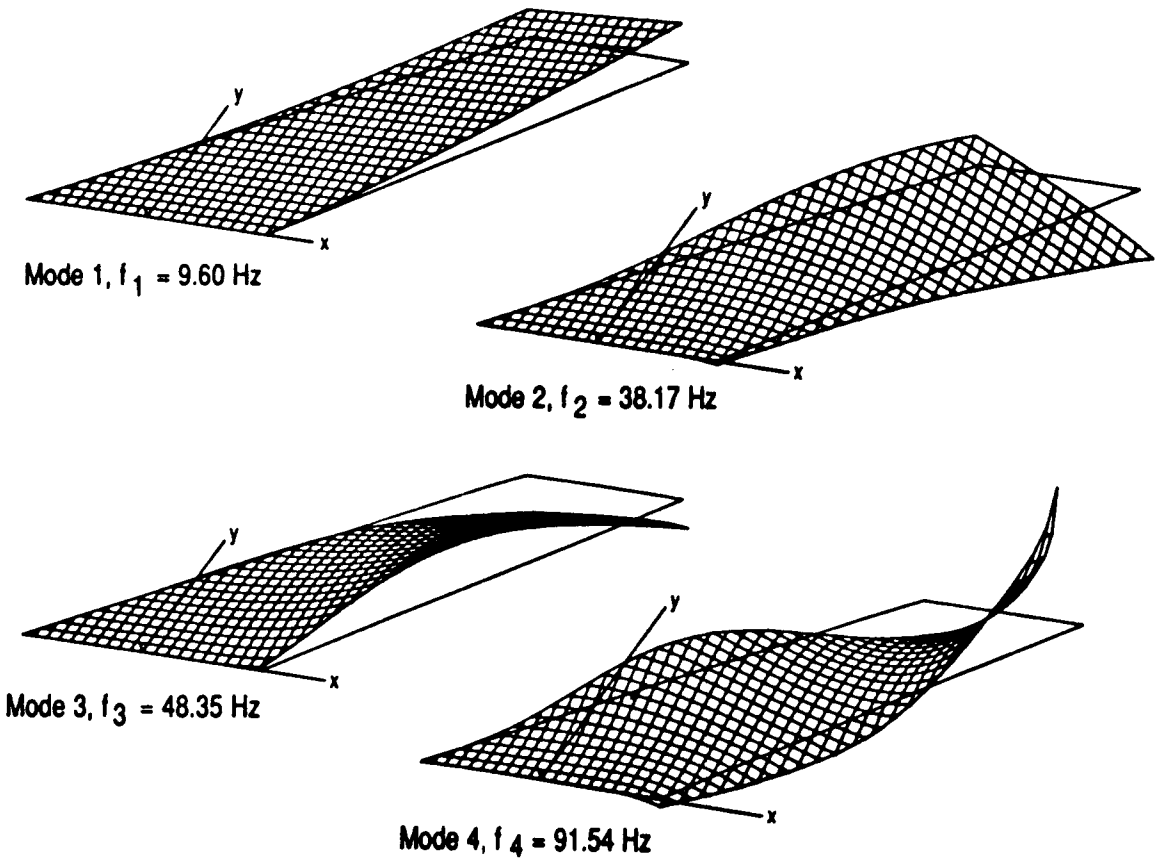

Fig. 6 Oblique projections of natural vibration modes of 45° sweptback wing.

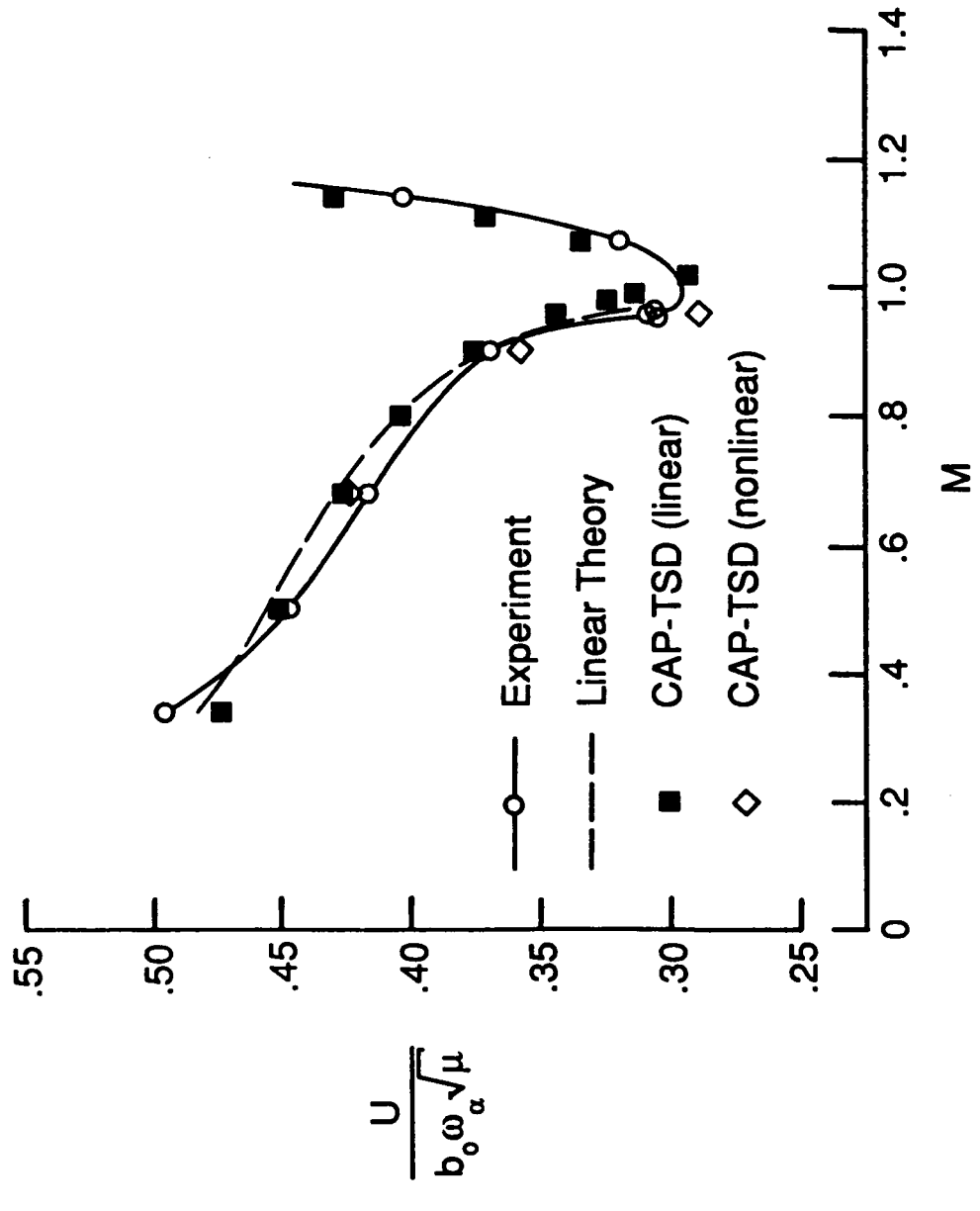

Fig. 7 Comparisons between calculated and experimental flutter speed index of the 45° sweptback wing.

NASA

National Aeronautics and Space Administration

Report Documentation Page

1. Report No.	2. Government Accession No.	3. Recipient's Catalog No.
NASA TM-100663		

4. Title and Subtitle
Recent Advances in Transonic Computational Aeroelasticity

5. Report Date
September 1988

6. Performing Organization Code

7. Author(s)
John T. Batina, Robert M. Bennett, David A. Seidel, Herbert J. Cunningham, Samuel R. Bland

8. Performing Organization Report No.

10. Work Unit No.
505-63-21-01

9. Performing Organization Name and Address
NASA Langley Research Center
Hampton, Virginia 22665-5225

11. Contract or Grant No.

13. Type of Report and Period Covered
Technical Memorandum

12. Sponsoring Agency Name and Address
National Aeronautics and Space Administration
Washington, DC 20546

14. Sponsoring Agency Code

15. Supplementary Notes
This paper will be presented at the Symposium on Advances and Trends in Computational Structural Mechanics and Fluid Dynamics, Washington, D.C., October 17-19, 1988.

16. Abstract

A transonic unsteady aerodynamic and aeroelasticity code called CAP-TSD has been developed for application to realistic aircraft configurations. The code permits the calculation of steady and unsteady flows about complete aircraft configurations for aeroelastic analysis in the flutter critical transonic speed range. The CAP-TSD code uses a time-accurate approximate factorization (AF) algorithm for solution of the unsteady transonic small-disturbance potential equation. The paper gives an overview of the CAP-TSD code development effort and presents results which demonstrate various capabilities of the code. Calculations are presented for several configurations including the General Dynamics one-ninth scale F-16C aircraft model and the ONERA M6 wing. Calculations are also presented from a flutter analysis of a 45^{0} sweptback wing which agree well with the experimental data. The paper presents descriptions of the CAP-TSD code and algorithm details along with results and comparisons which demonstrate these recent developments in transonic computational aeroelasticity.

17. Key Words (Suggested by Author(s))	18. Distribution Statement
Computational Aeroelasticity Unsteady Aerodynamics Flutter	Unclassified - Unlimited Subject Category - 02

19. Security Classif. (of this report)	20. Security Classif. (of this page)	21. No. of pages	22. Price
Unclassified	Unclassified	27	A03